# Rashba Effect of Polaron in RbCl Triangular Quantum Wells Under the Influence of Magnetic Field

Y.-L. Li[a] and S.-P. Shan[b,*]

[a] *College of Physics and Electronic Engineering, Jiangsu normal University, Xuzhou 221116, China*
[b] *College of Physics and Electromechanics, Fujian Longyan University, Longyan 364012, China*

Received: 29.01.2023 & Accepted: 24.05.2024

Doi: 10.12693/APhysPolA.146.129 *e-mail: ssping04@126.com

The Rashba effect of polaron in RbCl triangular quantum wells under the influence of a magnetic field is theoretically studied, and the expression of the ground state energy of the polaron is obtained within the Pekar variational method. The ground state energy of the polaron splits into two branches due to the Rashba effect. This phenomenon fully demonstrates that the influence of orbit and spin interaction in different directions on the energy of the polaron is not negligible. Because the contribution of the magnetic field cyclotron resonance frequency to the Rashba spin–orbit splitting is a positive value, the energy spacing becomes larger as the magnetic field cyclotron resonance frequency increases. Due to the spin–orbit coupling interaction, the energy splits at zero field. The total energy is reduced due to the presence of phonon. Therefore, the polaron state is more stable than the bare electron state, and the polaron energy splitting is more stable.

topics: Rashba effect, magnetic field, phonon, triangular quantum well

## 1. Introduction

With the rapid development of information technology, there is an increasing demand for faster, more stable, and more efficient information storage and processing equipment [1–3]. Spintronics, as a new information technology, has advantages that other technologies cannot replicate. For example, high speed, low power consumption, and high density can realize ultra-fast information transmission and processing, which provides new possibilities for fast computation and communication [4, 5]. The potential impact of spintronics on information technology makes it an active area of research in condensed matter physics.

An important branch of spintronics is the study of the Rashba spin–orbit coupling effect in low-dimensional quantum systems [6–8]. In particular, the Rashba effect in quantum well (QW) systems has been widely studied in recent years. For example, Zhao et al. [9] calculated the Rashba coefficient and Rashba spin splitting for the first subband of $Al_{0.6}Ga_{0.4}N/GaN/Al_{0.3}Ga_{0.7}N/Al_{0.6}Ga_{0.4}N$ QW, each as a function of the thickness of the inserted $Al_{0.3}Ga_{0.7}N$ layer and external electric field. Results show that the Rashba coefficient and the Rashba spin splitting in the $Al_{0.6}Ga_{0.4}N/GaN/Al_{0.3}Ga_{0.7}N/Al_{0.4}Ga_{0.4}N$ QW could be modulated by changing the relative thickness of GaN and $Al_{0.3}Ga_{0.7}N$ layers and the external electric field, thereby giving guidance for designing the spintronic devices. Li et al. [10] investigated theoretically the Rashba spin–orbit splitting of a hydrogenic donor impurity in GaAs/GaAlAs quantum wells by the framework of effective-mass envelope function theory. Resorting to an external gate potential, Meng et al. [11] explored the spin–orbit coupling in n-quantum well structures. Quantum-well structures from triple to septuple were constructed; the spin–orbit coupling coefficient of the lowest subband was always much larger than those of the other subbands, which led to greater spin splitting. Electron spin has also been experimentally studied, e.g., by Qiu and Gui et al. [12], who studied the giant Rashba effect in HgTe quantum wells with inverted energy bands. The spin–orbit splitting of III–V semiconductors is a linear term of momentum in the Hamiltonian of the system, which results in the dispersion relation of electron energy, and the energy is split from one parabola into two. The Rashba effect was previously considered to be caused by the electric field at the interface of the heterojunction, but it has been proven that the effect of the electric field on the Rashba effect is small, and the main contribution comes from the asymmetry of the wave function at the interface. In triangular quantum well, due to

the asymmetry of the lattice structure, there are special phenomena such as the spin–orbit coupling effect and rotational symmetry breaking of spin Hamiltonian. These phenomena make triangular quantum wells have a wide application prospect in spin transport and spin manipulation.

A lot of research has been done on the Rashba effect in the electronic systems, but there are few in the field of polaron. Using the linear combination operator method, Zhang et al. [13] studied the influence of Rashba spin–orbit interaction on the ground state energy of weakly coupled polaron in GaAs semiconductor triangular quantum wells. Due to the influence of the Rashba effect, the ground state energy of the polaron splits into two branches on the basis of zero spin. Within the improved linear combination operator method, Zhang [14] also investigated the Rashba spin–orbit splitting of the effective mass of strongly coupled polaron in RbCl semiconductor triangular quantum wells. The effective mass of polaron also splits under the Rashba spin–orbit interaction. In this paper, the Rashba effect of strongly coupled polaron in RbCl triangular quantum wells under the influence of a magnetic field is theoretically studied using the Landau–Pekar variational method.

## 2. Theoretical derivation

As shown in Fig. 1, a triangular quantum well composed of two polar media grows in the $z$-direction. We only consider an electron interacting with the bulk longitudinal optical phonon field and ignore the interaction between the electron and the interface optical phonon. Thus, the electron–phonon interaction forms a strongly coupled polaron. The strong coupling material RbCl with sphalerite structure is selected in the triangular quantum well. A magnetic field with vector potential $\boldsymbol{A} = B(-y/2, x/2)$ is applied along the $z$-direction. Considering the anisotropy of the sphalerite structure and using the effective mass approximation, we write the Hamiltonian of the system as

$$H = \frac{1}{2m}\left[\left(p_x - \frac{\bar{\beta}^2}{4}y\right)^2 + \left(p_y + \frac{\bar{\beta}^2}{4}x\right)^2\right] + \frac{p_z^2}{2m} + V(z) + \sum_{\boldsymbol{k}} \hbar\omega_{LO}\ \hat{\alpha}_{\boldsymbol{k}}^{\dagger}\hat{a}_{\boldsymbol{k}} + \sum_{\boldsymbol{k}}\left[V_k\, a_{\boldsymbol{k}} \exp\left(\mathrm{i}\boldsymbol{k}\cdot\boldsymbol{r}\right) + \mathrm{h.c.}\right] + \frac{\alpha_R}{\hbar}\left[\left(p_y + \frac{\bar{\beta}^2}{4}x\right)\sigma_x - \left(p_x - \frac{\bar{\beta}^2}{4}y\right)\sigma_y\right]. \quad (1)$$

Here, $\bar{\beta}^2 = \frac{2eB}{c}$. The electron band mass, electron momentum, and electron position vector are denoted by $m$, $\boldsymbol{p} = (p_x, p_y, p_z)$, and $\boldsymbol{r} = (\rho, z)$, respectively. We use $\hat{a}_{\boldsymbol{k}}^{\dagger}$ ($\hat{a}_{\boldsymbol{k}}$) to define the creation (annihilation) operator of a bulk longitudinal optical phonon with the frequency $\omega_{LO}$ and the wave vector $\boldsymbol{k}$. The Pauli matrix operator is replaced by $\boldsymbol{\sigma}$.

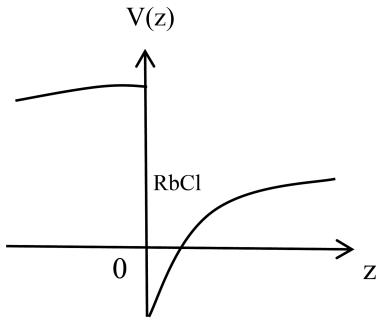


Fig. 1. Triangular quantum well structure.

The Rashba spin–orbit coupling parameter is represented by $\alpha_R$ and satisfies $\alpha_R = d\langle E\rangle$. Here, $d$ is related to many factors in semiconductor materials, and $\alpha_R$ is also linear with the expected value $\langle E\rangle$ of the self-built electric field.

The triangular potential is used to approximately replace the conduction band bending potential, which can be expressed as

$$V(z) = \begin{cases} eF_s z, & z > 0, \\ \infty, & z \le 0. \end{cases} \quad (2)$$

The built-in electric field is

$$F_s = \frac{4\pi e\, n_s}{\varepsilon_{01}}. \quad (3)$$

Here, $n_s$ refers to the surface density of the electron, and $\varepsilon_{01}$ is the static dielectric constant. The Fourier coefficients of the electron–phonon interaction are represented as

$$V_k = \mathrm{i}\left(\frac{\hbar\omega_{LO}}{k}\right)\sqrt[4]{\frac{\hbar}{2m\,\omega_{LO}}}\sqrt{\frac{4\pi\alpha}{V}}. \quad (4)$$

In (4), $V$ is the volume of the semiconductor, and $\alpha$ is the electron–phonon coupling strength, which depends on the material of the quantum well.

Under the adiabatic approximation, the unitary transformation is performed on (1), and the unitary transformation operator is introduced as follows

$$U = \exp\left[\sum_{\boldsymbol{k}}\left(\hat{a}_{\boldsymbol{k}}^{+} f_k - \hat{a}_{\boldsymbol{k}} f_k^*\right)\right]. \quad (5)$$

Here, $f_k$ and $f_k^*$ are variational parameter functions, which can be obtained through variational techniques. The transformed Hamiltonian is

$$H' = U^{-1}HU = \frac{1}{2m}\left[\left(p_x - \frac{\bar{\beta}^2}{4}y\right)^2 + \left(p_y + \frac{\bar{\beta}^2}{4}x\right)^2\right] + \frac{p_z^2}{2m} + eF_s z + \sum_{\boldsymbol{k}}\hbar\omega_{LO}\left(\hat{a}_{\boldsymbol{k}}^{\dagger} + f_k^*\right)\left(\hat{a}_{\boldsymbol{k}} + f_k\right) + \sum_{\boldsymbol{k}}\left[V_k\left(a_{\boldsymbol{k}} + f_k\right)\exp\left(\mathrm{i}\boldsymbol{k}\cdot\boldsymbol{r}\right) + \mathrm{h.c.}\right] + \frac{\alpha_R}{\hbar}\left[\left(p_y + \frac{\bar{\beta}^2}{4}x\right)\sigma_x - \left(p_x - \frac{\bar{\beta}^2}{4}y\right)\sigma_y\right]. \quad (6)$$

The ground state trial wave function of the system is selected as

$$|\psi\rangle = \sqrt{\frac{1}{2\pi}}\delta \mathrm{e}^{-\frac{\delta\rho}{2}} \sqrt{\frac{\beta'}{2}} z \mathrm{e}^{-\frac{\beta' z}{2}} \left(a\chi_{\frac{1}{2}} + b\chi_{-\frac{1}{2}}\right) |0\rangle_{\mathrm{ph}}, \tag{7}$$

where $|0\rangle_{\mathrm{ph}}$ is the unperturbed zero phonon state, which acts on the annihilation operator and satisfies $\hat{a}_{\boldsymbol{k}} |0\rangle_{\mathrm{ph}} = 0$. We define

$$\chi_{\frac{1}{2}} = \begin{pmatrix} 1 \\ 0 \end{pmatrix} \quad \text{and} \quad \chi_{-\frac{1}{2}} = \begin{pmatrix} 0 \\ 1 \end{pmatrix} \tag{8}$$

as the spin-up and spin-down states, respectively, where $\delta$ and $\beta'$ are variational parameters. The expected value of (6) with respect to $|\psi\rangle$ can be expressed as

$$F(f_k, f_k^*) = \langle\psi| H' |\psi\rangle . \tag{9}$$

Taking $\frac{\partial F}{\partial f_k} = 0$ and $\frac{\partial F}{\partial f_k^*} = 0$, we get

$$f_k^* = -\frac{V_k \langle\psi| \mathrm{e}^{\mathrm{i}\boldsymbol{k}\cdot\boldsymbol{r}} |\psi\rangle}{\hbar\omega_{LO}} \tag{10}$$

and

$$f_k = -\frac{V_k^* \langle\psi| \mathrm{e}^{-\mathrm{i}\boldsymbol{k}\cdot\boldsymbol{r}} |\psi\rangle}{\hbar\omega_{LO}}. \tag{11}$$

Substituting $f_k$ and $f_k^*$ into (9) and replacing the sum with an integral, we obtain the total energy of the system

$$E = \frac{\hbar^2 k^2}{2m} + \frac{3m\omega_c^2}{4\delta^2} + \frac{\beta'^2\hbar^2}{8m} + \frac{12\pi n_s e^2}{\beta'\varepsilon_{01}} - \frac{3\pi}{16}\alpha\hbar\omega_{LO}\delta\sqrt{\frac{\hbar}{2m\omega_{LO}}} \pm \alpha_R\left(k + \frac{m\omega_c}{\hbar\delta}\right). \tag{12}$$

Here, $\omega_c = \frac{eB}{mc}$ is defined as the magnetic cyclotron resonance frequency.

## 3. Numerical calculation

From (12), we find that the polaron energy experiences splitting. In Fig. 1, the structural inversion asymmetry of the triangular quantum well results in the electron spin degeneracy being dissolved, resulting in the electron energy at the Feimi surface experiencing Rashba spin–orbit splitting. Although the spin splitting caused by bulk inversion asymmetry exists in polar semiconductors, it is mainly caused by structural inversion asymmetry for narrow-band gap semiconductor. We selected the narrow-band gap semiconductor RbCl as the strong coupling material in the well. The corresponding parameters for RbCl are $\hbar\omega_{LO} = 22.317$ meV, $m = 0.432\,m_0$, $\omega_{LO} = 3.39\times10^{13}$ s$^{-1}$, $\alpha = 4.2$. Here, $m_0$ is the free electron mass. In order to more clearly illustrate the influence of wave vector, magnetic field cyclotron resonance frequency, and electron surface density on the Rashba spin–orbit splitting, the ground state energy of the strongly coupled polaron in a triangular quantum well is numerically calculated. The numerical conclusions are shown in Figs. 2–6. The numerical values used in the calculation have been selected within the valid value range of each physical quantity.

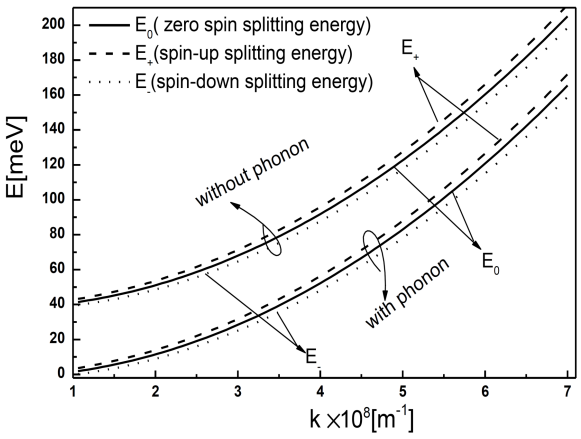


Fig. 2. The relationship between ground state energy $E$ and wave vector $k$ with phonon and without phonon.

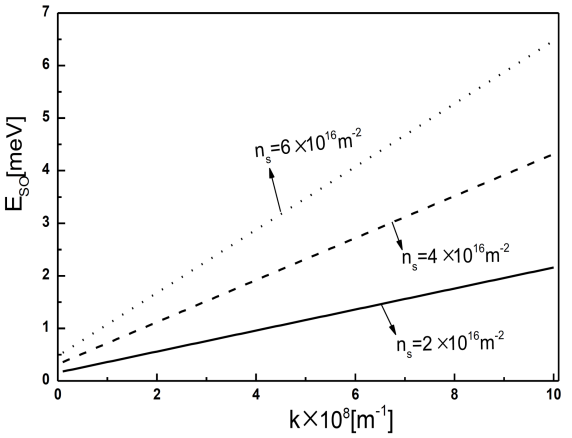


Fig. 3. The relational curves between the spin splitting energy $E_{so}$ and the wave vector $k$ when the electron surface density $n_s$ takes different values.

For fixed $\omega_c = 4\times10^{13}$ s$^{-1}$, $n_s = 3\times10^{16}$ m$^{-2}$, $\alpha_R = 0.8\times10^{-8}$ meV m, the relationship between the ground state energy $E$ and the wave vector $k$ with phonon and without phonon is depicted in Fig. 2. Due to the influence of Rashba spin–orbit interaction, the ground state energy is split into two branches on the basis of zero spin. The solid lines represent the zero spin splitting energy $E_0$, the short solid lines represent the spin-up splitting energy $E_+$, and the dotted lines represent the spin-down splitting energy $E_-$. The split distance increases with the increase in the wave vector. In Fig. 2, the ground state energy is an increasing function of the wave vector. It can be seen from the trend of the curve that the contribution of $k^2$ is greater than that of $k$ in (12). Figure 3 shows the respective curves of the

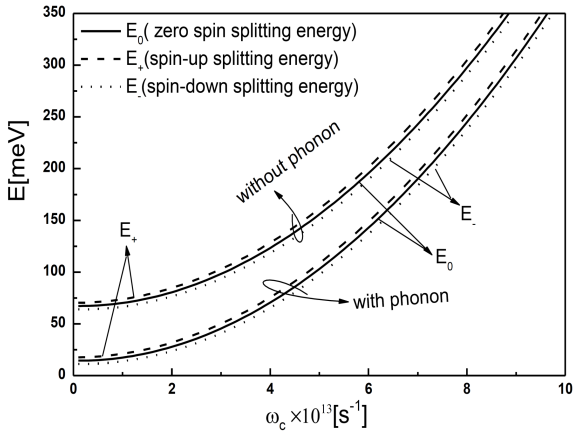


Fig. 4. The relationship between the ground state energy $E$ and the magnetic field cyclotron resonance frequency $\omega_c$ with phonon and without phonon.

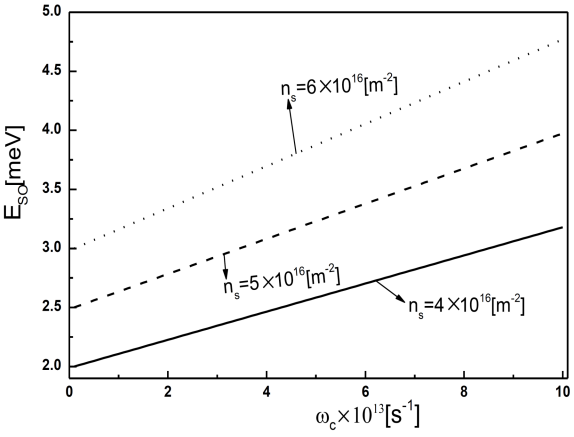


Fig. 5. The relational curves between the spin splitting energy $E_{so}$ and the magnetic field cyclotron resonance frequency $\omega_c$ when the electron surface density $n_s$ takes different values.

Rashba spin–orbit splitting energy $E$ as a function of the wave vector $k$, with the electron surface density $n_s$ taken as $2\times10^{16}$, $4\times10^{16}$, and $6\times10^{16}$ m$^{-2}$. It is found that the spin–orbit splitting energy increases linearly with the increase in the wave vector. In the expression for the Rashba spin–orbit splitting energy $E_{so} = 2\alpha_R(k + \frac{m\omega_c}{\hbar\delta})$, the wave vector is proportional to the Rashba spin–orbit splitting energy, so the Rashba spin–orbit splitting energy is an increasing function of the wave vector. It is also seen in Fig. 3 that the energy still splits for the wave vector $k = 0$. This is caused by the influence of the magnetic field on the spin–orbit interaction. As the wave vector increases, the curve spacing increases. This indicates that the larger the wave vector is, the more significant the energy splitting is. This is consistent with the conclusion from Fig. 2.

Figure 4 shows the relational curve between the ground state energy $E$ and the magnetic field cyclotron resonance frequency $\omega_c$ with phonon and without phonon, for fixed $k = 4\times10^8$ m$^{-1}$, $n_s = 4\times10^{16}$ m$^{-2}$, $\alpha_R = 0.8\times10^{-8}$ meV m. Due to the Rashba effect, the ground state energy splits up and down into two branches on the basis of zero spin. The solid lines represent the zero spin splitting energy $E_0$, the short solid lines represent the spin-up splitting energy $E_+$, and the dotted lines represent the spin-down splitting energy $E_-$. As can be seen from the figure, the ground state energy increases parabolically with the increase in the magnetic field cyclotron resonance frequency. The applied magnetic field means that the electron is subject to a new constraint, resulting in a large overlap of the electron wave functions in the well. Thus, the electron–phonon interaction is enhanced with the enhancement of the magnetic field. The expression of the magnetic field cyclotron resonance frequency is $\omega_c = \frac{eB}{mc}$, i.e., the magnetic field cyclotron resonance frequency is proportional to the magnetic field strength, so the ground state energy increases with the increase in the magnetic field cyclotron resonance frequency. When the magnetic cyclotron resonance frequency $\omega_c = 0$, the energy still splits. It is the zero magnetic field spin splitting of the electron caused by the Rashba spin–orbit interaction. However, with the increase in the magnetic field cyclotron resonance frequency, the change in the energy spacing is not obvious. Compared with Fig. 2, the magnetic field cyclotron resonance frequency has less influence on Rashba spin–orbit splitting energy than the wave vector.

Figure 5 shows the relationship between the Rashba spin–orbit splitting energy and the magnetic field cyclotron resonance frequency when the electron surface density $n_s$ is assigned to $2\times10^{16}$, $4\times10^{16}$, and $6\times10^{16}$ $m^{-2}$. In the figure, the spin–orbit splitting energy increases linearly with the increase in the magnetic field cyclotron resonance frequency. In the expression $E_{so} = 2\alpha_R(k + \frac{m\omega_c}{\hbar\delta})$ for the Rashba spin–orbit splitting energy, the contribution of the magnetic field cyclotron resonance frequency to the spin–orbit splitting energy is positive, and $E_{so}$ is proportional to $\omega_c$. It is also found from Fig. 5 that the curve spacing increases slowly with the change in $\omega_c$. This conclusion is consistent with Fig. 4, indicating that the effect of magnetic field cyclotron resonance frequency on the spin splitting energy is relatively small. From the expression of the spin splitting energy, we can see that the contribution of the magnetic field cyclotron resonance frequency to the spin splitting energy is positive, so the energy spacing will increase with the increase in the magnetic field cyclotron resonance frequency.

For fixed $k = 3\times10^8$ m$^{-1}$ and $\omega_c = 5\times10^{16}$ s$^{-1}$, the functional relationship between the ground state energy $E$ and the electron surface density $n_s$ with phonon and without phonon is shown in Fig. 6. Due to the Rashba effect, the ground state energy splits

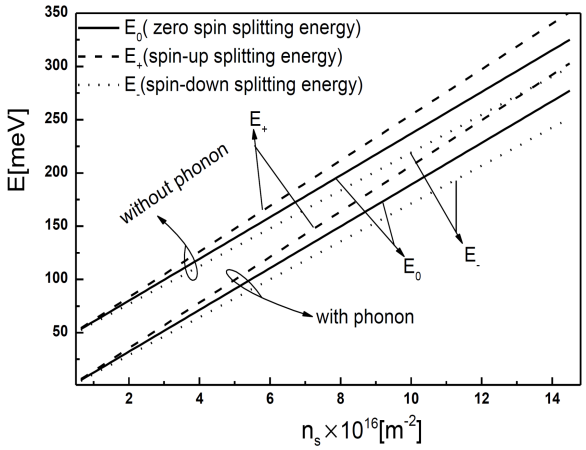


Fig. 6. The relationship between the ground state energy $E$ and the electron surface density $n_s$ with phonon and without phonon.

up and down into two branches on the basis of zero spin. The solid lines represent the zero spin splitting energy $E_0$, the short solid lines represent the spin-up splitting energy $E_+$, and the dotted lines represent the spin-down splitting energy $E_-$. In Fig. 6, the ground state energy is an increasing function of the electron surface density. It can be seen from (2) and (3) that the conduction band bending increases with the increase in electron surface density. The electron moves away from the interface, which leads to enhanced electron–phonon interaction. Therefore, the ground state energy increases with the increase in electron surface density. It is also found that when the electron surface density $n_s = 0$, the ground state energy is constant, i.e., the energy does not split. The energy spacing increases with the increase in electron surface density. The spin–orbit coupling parameter satisfies $\alpha_R = d\langle E\rangle$ and at the same time $\langle E\rangle = e\,n_s/\varepsilon_{01}$, so the spin–orbit coupling parameter is proportional to the electron surface density. When the electron surface density $n_s$ equals zero, the Rashba spin–orbit coupling parameter is zero, and the energy does not split. The spin–orbit coupling parameter is proportional to the electron surface density, so the energy spacing increases as the electron surface density increases. In Figs. 2 and 4, when the wave vector and the magnetic field cyclotron resonance frequency are fixed, the larger the electron surface density is, the larger the spin splitting energy is. This conclusion is consistent with Fig. 5.

The energy splitting caused by the Rashba spin–orbit interaction is due to the inversion asymmetry of the crystal structure. An applied magnetic field can also cause the Zeeman splitting of the energy. However, the energy splitting caused by the Rashba spin–orbit interaction is more pronounced in narrow band gap semiconductors. In order to more clearly represent the effect of the magnetic field on the Rashba spin–orbit splitting, we only consider the Rashba effect and ignore the Zeeman effect. From Figs. 2, 4, and 6, it is found that the particle energy with phonon is smaller than that without phonon. The electron–phonon interaction reduces the total energy of the particle, so the polaron state is more stable than the bare electron state, and the polaron splitting is more stable.

## 4. Conclusions

Using the Landau–Pekar variational method, we studied the Rashba effect of polaron RbCl triangular quantum wells under the influence of a magnetic field. The expression of the ground state energy of the polaron is obtained by theoretical derivation. The results show that the polaron energy is related not only to the wave vector and the electron surface density, but also to the magnetic field cyclotron resonance frequency. We discussed the relations among the ground state energy of the polaron with the wave vector, the electron surface density, and the cyclotron resonance frequency of the magnetic field by numerical calculation. Due to the Rashba effect, the ground state energy of the polaron splits into two branches. This phenomenon fully demonstrates that the influence of orbit and spin interaction in different directions on the energy of the polaron is not negligible. Because the contribution of the magnetic field cyclotron resonance frequency to the Rashba spin–orbit splitting is a positive value, the energy spacing becomes larger as the magnetic field cyclotron resonance frequency increases. Due to the spin–orbit coupling interaction, the energy splits at zero field. The presence of phonons reduces the total energy of the particles, so the polaron is more stable than the bare electron state, and the energy splitting is more stable.

## References

[1] E.I. Rashba, Al.L. Efros, *Phys. Rev. Lett.* **91** 126405 (2003).

[2] D.D. Awschalom, R.A. Buhrman, J.M. Daughton, S. von Molnár, M.L. Roukes, A.Y. Chtchelkanova, D.M. Treger, *Science* **294**, 1488 (2000).

[3] J. Lee, H.N. Spector, *J. Appl. Phys.* **99**, 113708 (2006).

[4] S.P. Shan, S.H. Chen, J.L. Xiao, *J. Low Temp. Phys.* **176**, 93 (2014).

[5] S.-P. Shan, S.-H.Chen, *J. Low Temp. Phys.* **197**, 379 (2019).

[6] E. Sadegh, Gh. Rezaie, *Pramana J. Phys.* **75**, 749 (2010).

[7] R. Ferdous, K.W. Chan, M. Veldhorst, J.C.C. Hwang et al., *Phys. Rev. B* **97**, 241401 (2018).

[8] L. Hong, J. Ge, S. Shuang, D.-K. Liu, *Acta Phys. Sin.* **71**, 016301 (2022).

[9] Z.-Y. Zhao, H.-L. Wang M. Li, *Acta Phys. Sin.* **65**, 097101 (2016).

[10] S.-S. Li, J.-B.Xia, *Nanoscale Res. Lett.* **4**, 178 (2009).

[11] F. Meng, J. Zhao, J. Cheng, W. Liu, *Phys. B* **649**, 414468 (2023).

[12] Z.-J. Qiu, Y.-S. Gui, X.-Z. Shu, N.Dai et al., *Acta Phys. Sin.* **53**, 1186 (2004).

[13] Z. Hairui, S. Yong, *J. Semicond* **35**, 102001 (2014).

[14] Z. Hai-Rui, X. Jing-Lin, *Commun. Theor. Phys.* **50**, 995 (2008).